A porous flow model of flank eruptions on Mt. Etna: second-order perturbation theory

Maurizio Bonafede and Nicola Cenni
Dipartimento di Fisica, Settore di Geofisica, Università di Bologna, Italy

Abstract
A porous flow model for magma migration from a deep source within a volcanic edifice is developed. The model is based on the assumption that an isotropic and homogeneous system of fractures allows magma migration from one localized feeding dyke up to the surface of the volcano. The maximum level that magma can reach within the volcano (*i.e.*, the «free surface» of magma, where fluid pressure equals the atmospheric pressure) is reproduced through a second-order perturbation approach to the non-linear equations governing the migration of incompressible fluids through a porous medium. The perturbation parameter is found to depend on the ratio of the volumic discharge rate at the source (m^3/s) divided by the product of the hydraulic conductivity of the medium (m/s) times the square of the source depth. The second-order corrections for the free surface of Mt. Etna are found to be small but not negligible; from the comparison between first-order and second-order free surfaces it appears that the former is higher near the summit, slightly lower at intermediate altitudes and slightly higher far away from the axis of the volcano. Flank eruptions in the southern sector are found to be located in regions where the topography is actually lower than the theoretical free surface of magma. In this sector, modulations in the eruption site density correlate well with even minor differences between free surface and topography. In the northern and western sectors similar good fits are found, while the NE rift and the eastern sector seem to require mechanisms or structures respectively favouring and inhibiting magma migration.

Key words *volcanoes – magma migration – porous medium – flank eruptions*

1. Introduction

Small volcanoes often exhibit conical shapes which can be generally ascribed to the presence of a centre of symmetry, provided by a localized and persistent source of magma. In similar instances, soil mechanics or rock mechanics theory predict gently concave shapes with circular cross sections (Milne, 1878-1879; Becker, 1885; Shteynberg and Solov'yev, 1976). However, explosive volcanism, calderic collapses, gravity instability and changes in the location of lava sources make this conical shape a very rough approximation of real volcanoes.

For larger composite volcanoes, which are characterized by several vents and frequent flank eruptions, Lacey *et al.* (1981) proposed that their geometrical forms may be determined by the hydraulic resistance met by magma flowing through an isotropic matrix of pre-existing conduits. They assumed that the topographical surface of a volcano is at constant fluid pressure and applied the Dupuit approximation (*e.g.*, Bear 1976) to model the transient evolution of the top surface of magma in terms of unconfined flow within a porous

Mailing address: Prof. Maurizio Bonafede, Dipartimento di Fisica, Settore di Geofisica, Università di Bologna, Viale C. Berti Pichat 8, 40127 Bologna, Italy; e-mail: bonafede@ibogfs.df.unibo.it

medium. Bonafede and Boschi (1992) reformulated the porous flow model in order to circumvent objections raised by Wadge and Francis (1982); they employed a different scheme of solution (perturbation approach) and proposed a probabilistic interpretation for the porous flow model and the free surface of magma. According to Bonafede and Boschi (1992) it is not the shape of a volcano that can be reproduced by the free surface of magma, since several factors (other than lava field emplacements) control the topography (*e.g.*, Williams and McBirney, 1979). The free surface can be rather employed to describe the altitude reached, on the average, by magma penetrating along different paths, for a given output rate at the source.

The porous flow model emphasizes the role of fluid pressure which drives the flow against viscous friction and gravity, thus determining the maximum level attainable from the fluid within an isotropic and homogeneous permeable medium.

According to the previous considerations, modeling magma dynamics within large volcanoes in terms of a porous flow model does not seem inappropriate, if the dimension and spacing of fractures are small compared with the characteristic dimension of the volcano, if the fluid is Newtonian and the flow is laminar. In such cases, fluid flow is directly proportional to the pressure gradient along a dyke and inversely proportional to fluid viscosity, as provided by Darcy's law in fluid saturated permeable media. Furthermore, different flank eruptions may be interpreted, in the context of magma-driven crack propagation, as the result of magma penetrating along several possible paths starting from a main source. If we average the magma migration over several flank eruptions, we expect the resulting behaviour to be similar to that provided by Darcy's flow through a permeable rock matrix (this assumption is equivalent to assessing that an average over time may be statistically equivalent to an average over all admissible system configurations).

On Mt. Etna the assumptions made above seem to be generally acceptable; several detailed morpho-tectonic studies (*e.g.*, Cristofolini *et al.*, 1978, 1981; Lo Giudice *et al.*, 1982; Rasà, 1982) show that eruptive fractures are widespread and generally related to a tensional stress field inside the volcano. There are however regions characterized by an anomalous density of fractures, the most notable being the NE rift, coinciding with an ancient buried caldera rim.

In the following we shall assume that a point source of magma is buried within the crust. This source simulates a location from which several interconnected channels are assumed to permit magma migration to the surface when a sufficient over-pressure is available. We shall derive the solution governing the transient evolution of the free surface of magma, to second order in a perturbation approach.

2. Equations

The flow of a homogeneous and incompressible fluid with density d and viscosity μ, subject to gravity g, through a solid (incompressible) matrix characterized by permeability k, is governed by Darcy's law:

$$f = -K \nabla \Phi, \tag{2.1}$$

where f is the volumetric flow rate, Φ is the piezometric head, and K is the hydraulic conductivity, respectively defined as

$$\Phi = z + \frac{p}{dg}, \qquad K = \frac{kdg}{\mu} \tag{2.2}$$

(p is the fluid pressure and z is the vertical coordinate, positive upwards). The locus where the fluid pressure equals the atmospheric pressure within the porous matrix is called «free surface» (phreatic surface, in hydrology). We shall take the atmospheric pressure as the reference for fluid pressure, so that fluid pressure is assumed to vanish at the free surface. The depth of the free surface is then characterized by the implicit equation:

$$\Phi(x, y, z, t) = z \quad \rightarrow \quad z = Z(x, y, t). \tag{2.3}$$

Mass conservation for an uncompressible fluid furthermore requires that, away from sorces or sinks of fluid,

$$\nabla^2 \Phi = 0. \tag{2.4}$$

In order to complete the specification of the problem, boundary conditions must be specified. The free surface condition can be stated as a non-linear equation for Φ over the surface $z = Z(x, y, t)$ (*e.g.*, Bear, 1976, case without accretion):

$$n_e \frac{\partial \Phi}{\partial t} = K\left[\left(\frac{\partial \Phi}{\partial x}\right)^2 + \left(\frac{\partial \Phi}{\partial y}\right)^2 + \left(\frac{\partial \Phi}{\partial z}\right)^2\right] - K\frac{\partial \Phi}{\partial z},$$

$$\text{on} \quad z = Z(x, y, t), \tag{2.5}$$

where n_e is the effective porosity (total porosity minus unconnected porosity). This condition is assigned over the free surface $z = Z(x, y, t)$, which is unknown *a priori*. Once a solution is known for the potential Φ, the free surface $z = Z(x, y, t)$ can be obtained from the condition (2.3).

The unconfined flow problem is characterized by redundant boundary conditions – eq. (2.3) and the non-linear condition (2.5) – to be imposed on a surface which is *a priori* unknown. Accordingly, the flow domain is *a priori* unknown and the problem cannot be tackled employing standard numerical methods. Exact analytical solutions are generally unavailable and resort must be made to methods of approximations.

Bonafede and Boschi (1992) assume that a point-source of fluid is present for time $t > 0$, at depth $z = -z_0$, in $x = y = 0$, emitting a constant upward flow rate of $2\pi q$ cubic meters of fluid per unit time, across an otherwise impervious basement: this last condition imposes the additional boundary condition

$$\frac{\partial \Phi}{\partial z} = 0 \quad \text{on} \quad z = -z_0.$$

The following non-dimensional quantities can be profitably employed

$$\boldsymbol{r} = \left(\frac{x}{z_0}, \frac{y}{z_0}, \frac{z}{z_0}\right), \quad \rho = \frac{\sqrt{x^2 + y^2}}{z_0}, \quad \eta = \frac{z}{z_0},$$

$$\tau = \frac{Kt}{n_e z_0}, \quad Q = \frac{q}{K z_0^2}, \quad \varphi = \frac{\Phi}{z_0}, \quad \zeta = \frac{Z}{z_0} \tag{2.6}$$

to denote, respectively, the position vector, horizontal distance, vertical coordinate, time, non-dimensional emission rate, hydraulic potential and free surface.

The mass conservation eq. (2.4) can be rewritten (taking the source in $\boldsymbol{r} = \boldsymbol{r}_s$ into account), as

$$\nabla^2 \varphi = -4\pi Q \delta(\boldsymbol{r} - \boldsymbol{r}_s).$$

As described in Bear (1976), the perturbation approach of Polubarinova-Kochina (1962) is employed in the following, expanding φ and ζ with respect to a perturbation parameter, which in the present case can be identified as Q (see also Bonafede and Boschi, 1992):

$$\begin{aligned} \varphi(x, y, z, t) &= \varphi_0(x, y, z, t) + Q\,\varphi_1(x, y, z, t) + \\ &+ Q^2 \varphi_2(x, y, z, t) + \mathrm{o}(Q^3), \\ \zeta(x, y, t) &= \zeta_0(x, y, t) + Q\,\zeta_1(x, y, t) + \\ &+ Q^2 \zeta_2(x, y, t) + \mathrm{o}(Q^3), \end{aligned} \tag{2.7}$$

where $\mathrm{o}(Q^3)$ denotes terms of order greater than 2, which will be neglected. Inserting (2.7) into (2.4) and (2.5) and equating equal powers of Q, we obtain a sequence of «sub-problems», in which the equations at order n require the knowledge of solutions at order $n-1$ (*e.g.*, Bear, 1976).

As in Bonafede and Boschi (1992), we impose the initial condition $\zeta = 0$ at $\tau = 0$; this will be assumed also as the zero-order free surface $\zeta_0 = 0$. Accordingly, φ_0 also vanishes, and the zero-order equations are identically satisfied. The first-order «sub-problem» is then

$$\begin{aligned}
&\nabla^2\varphi_1 = -4\pi\delta(\boldsymbol{r}-\boldsymbol{r}_s),\\
&\text{in}\quad -1<\eta\le 0,\quad \rho\ne 0\quad \text{if}\quad \eta=-1,\\
&\frac{\partial\varphi_1}{\partial\tau} = -\frac{\partial\varphi_1}{\partial\eta}\quad \text{on}\quad \eta=0,\\
&\text{and}\quad \frac{\partial\varphi_1}{\partial\eta}=0\quad\text{on}\quad \eta=-1,\\
&\varphi_1=0\quad\text{at}\quad\tau=0,\\
&\zeta_1=\varphi_1\quad\text{on}\quad\eta=0,
\end{aligned}\tag{2.8}$$

where $\delta(\boldsymbol{r}-\boldsymbol{r}_s)$ is Dirac's delta function and $\boldsymbol{r}_s$ is the source non-dimensional position $\boldsymbol{r}_s = (0, 0, -1)$. The second-order corrections are governed by:

$$\begin{aligned}
&\nabla^2\varphi_2 = 0,\qquad -1<\eta\le 0,\\
&\frac{\partial\varphi_2}{\partial\tau} + \frac{\partial\varphi_2}{\partial\eta} = \ell(\rho,\eta,\tau)\quad\text{on}\quad\eta=0,\\
&\text{and}\quad\frac{\partial\varphi_2}{\partial\eta}=0\quad\text{on}\quad\eta=-1\\
&\varphi_2=0\quad\text{at}\quad\tau=0\\
&\zeta_2=\varphi_1\frac{\partial\varphi_1}{\partial\eta}+\varphi_2\quad\text{on}\quad\eta=0,
\end{aligned}\tag{2.9}$$

where

$$\ell(\rho,\eta,\tau) = \varphi_1\frac{\partial}{\partial\eta}\left(-\frac{\partial\varphi_1}{\partial\eta}-\frac{\partial\varphi_1}{\partial\tau}\right)+(\nabla\varphi_1)^2.$$

The first-order correction was obtained by Bonafede and Boschi (1992) as:

$$\varphi_1(\rho,\eta,\tau) = \int_0^{+\infty} J_0(s\rho)\cdot \tag{2.10}$$
$$\cdot\left[A(s,\tau)\,e^{s\eta} + A(s,\tau)\,e^{-2s-s\eta} + e^{-s(\eta+1)}\right]ds$$

where J_0 is the Bessel function and

$$A(s,\tau) = \frac{e^{-s}}{1-e^{-2s}}\left[1-\frac{2}{1+e^{-2s}}\,e^{-s\tau\tanh s}\right].$$

This solution is employed in the next section to compute second-order corrections.

3. Second-order corrections to the free surface

In Bonafede and Boschi (1992) the free surface of magma for Mt. Etna was computed employing a first-order perturbation approach. In the present section the first-order solution will be employed in an iterative scheme of solution to obtain second-order corrections $\zeta_2(\rho,\tau)$ to the free surface.

The solution of the second-order problem (2.9) above can be obtained employing the Green function technique (Dagan, 1966). The cumbersome computational details are omitted (see Cenni, 1996). The formal solution for $\zeta_2(\rho,\tau)$ under the initial and boundary conditions specified above, is

$$\varphi_2(\rho,0,\tau) = \int_0^{+\infty} ds\int_0^{+\infty} d\rho'\int_0^{\tau} d\tau'\cdot$$
$$\cdot\left\{s\rho' J_0(s\rho)\,J_0(s\rho')\,e^{-s\tau'\tanh s}\,\ell(\rho',\tau-\tau')\right\}.$$

The function $\ell(\rho,\tau)$ is given after eq. (2.9) in terms of the first-order integral solution for φ_1. Accordingly, the formal solution is given in terms of a five-dimensional integral. Only two integrations can be performed analytically; the three remaining ones were performed numerically, after removing analytically the singular terms, employing suitable integrations by parts.

The first- and second-order terms ζ_1 and ζ_2 in the perturbation solution for the free surface are shown in fig. 1a,b for a few values of the non-dimensional time τ. The dimensional height of the free surface, corrected to second order, is given by

$$Z(\rho,\tau) = z_0\,(Q\zeta_1 + Q^2\zeta_2).\tag{3.1}$$

Clearly, the perturbation approach is justified

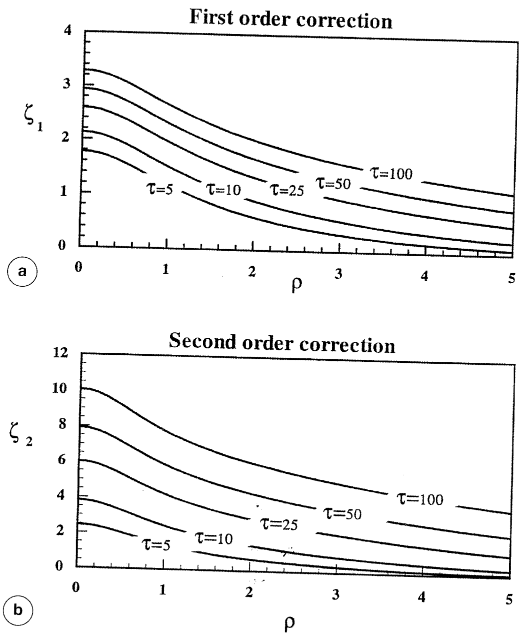

Fig. 1a,b. Non-dimensional first-order (a) and second-order (b) contributions to the free surface of a fluid in the presence of a unit point source at depth. The non-dimensional time τ noted next to each curve is defined in (2.6).

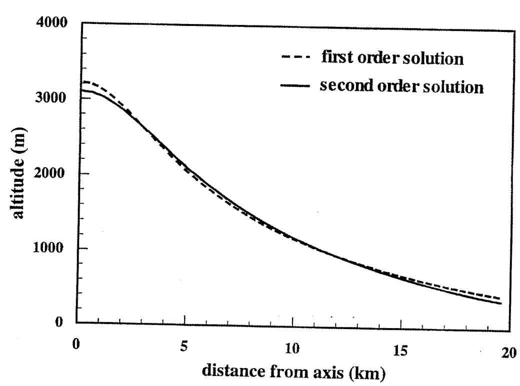

Fig. 2. Comparison between the first-order (dashed) and second-order (solid) free surfaces which provide the best-fit to Mt. Etna topography along the eruptive segment of the SSE section. For the first-order surface $\tau = 19$, $Q = 0.32$, $z_0 = 4500$ m, $h_0 = 400$ m. For the second-order surface $\tau = 10$, $Q = 0.22$, $z_0 = 5150$ m, $h_0 = 200$ m.

only if $Q \ll 1$, when second-order corrections are much less than first-order contributions.

4. Discussion of results

The free parameters Q, z_0 and τ appearing in the first-order approximation to the free surface, $Z \simeq Qz_0\zeta_1$, were determined by Bonafede and Boschi (1992) through a least-squares fit with the topography of Mt. Etna along the S-SE sector, where eruptive activity is present from the summit down to 500 m altitude. The same technique is employed here for the second-order approximation (3.1).

We searched for parameter values that minimize the misfit function F^2 along the S-SE section of Mt. Etna:

$$F^2 = \sum_{i=1}^{N} \frac{w_i\,(h_i - [Z_i - h_0])}{N},$$

where w_i is the weight associated with the i-th point along the S-SE section, Z_i is the height of the free surface as given by the second-order approximation (3.1), h_i is the topographical altitude and h_0 is the depth of the zero-order free surface ($z = 0$) below sea level. We assume $w_i = 1$ for points inside areas affected by eruptive activity (taken from Guest and Murray, 1979), $w_i = 0$, otherwise.

Figure 2 shows the best-fit free surfaces as computed from the first-order (dashed) and the second-order (solid) solutions. Slight differences between the two solutions are limited to the summit and to distal areas, where the first-order free surface is higher than the second-order one.

A remarkably good fit between the free surface and the topography of the S-SE sector (fig. 3a) is obtained for the following parameter values:

$$\tau = 10, \quad Q = 0.22, \quad z_0 = 5150 \text{ m}, \quad h_0 = 200 \text{ m}.$$

The comparison between the theoretical free surface and several radial sections of Mt. Etna is shown in fig. 3a-f. Along most sections, the comparison between the second-order free surface and the topography generally confirms the results obtained from the first-or-

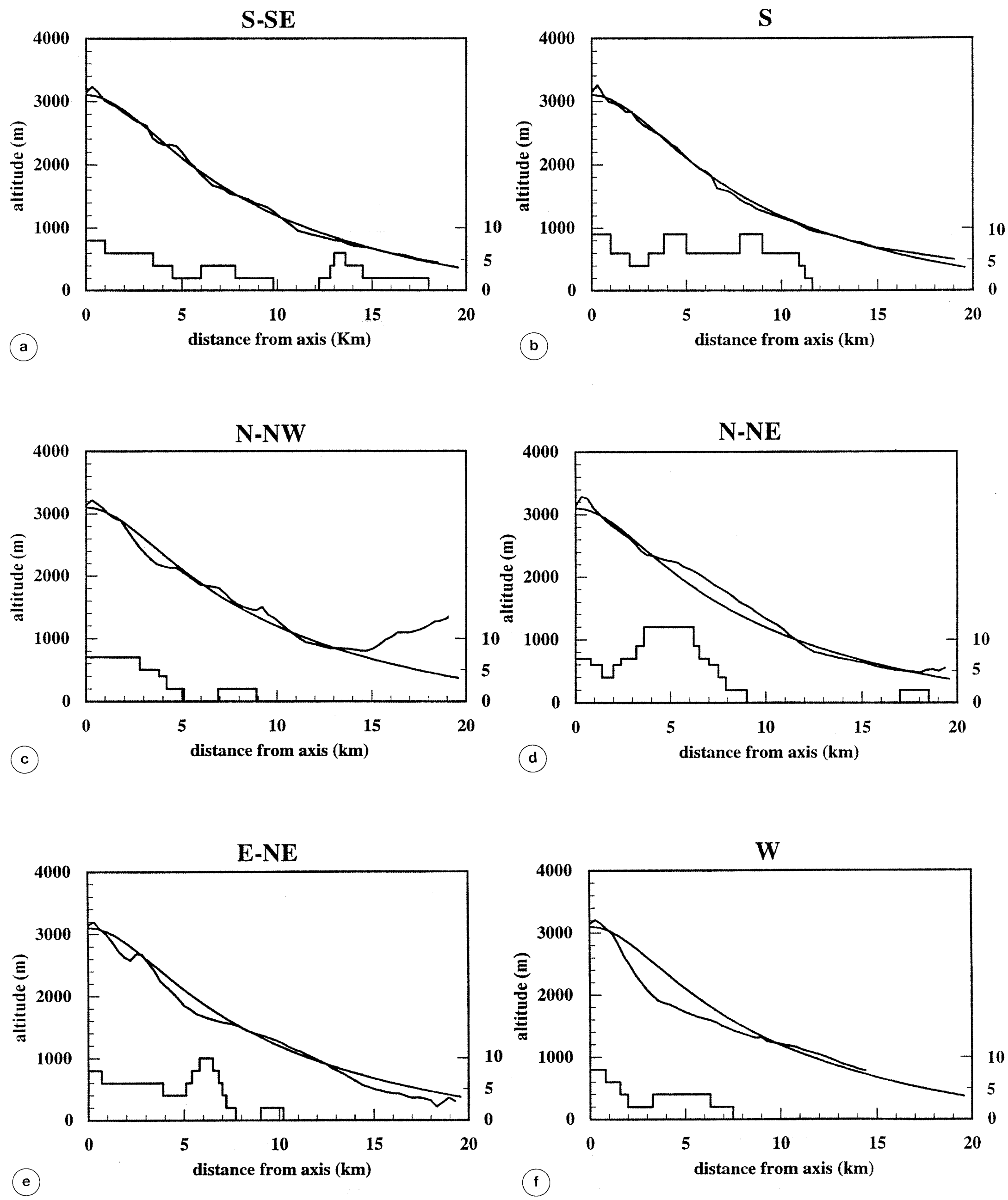

Fig. 3a-f. Comparison between the altitudes of best-fit second-order free surface (smooth line) and several topographic sections of Mt. Etna. The density distribution (per 4 km^2) of eruptive sites along the abscissas is taken from Guest and Murray (1979) (scale on the right).

der solution. It is worthwhile mentioning that the best-fit value obtained for the source depth ($z_0 + h_0 = 5350$ m) fits remarkably well with the depth of the Iblean platform below Mt. Etna, inferred as ~ 5000 m from seismic and structural studies (*e.g.*, Borgia *et al.*, 1992).

Figure 4a,b shows the detailed fracture patterns for two recent eruptions (in 1981 and 1928) characterized by extended fractures and large lava flows that threatened or destroyed villages at the base of the volcanic edifice (*e.g.*, Romano, 1982; Romano and Sturiale, 1982; Chester *et al.*, 1985). Figure 4a displays the 1981 fracture system which threatened the city of Randazzo. The lowest eruptive fissure outpoured a large flow of low-viscosity lava which in a few days reached the base of the volcanic edifice. When the lowest fracture segment became active, the flow from the upper segments ceased: this agrees with the present model, since in this way magma found an easier path to the surface, against gravity and viscous forces. It is to be mentioned that the previous lava flow in this area took place in 1536,

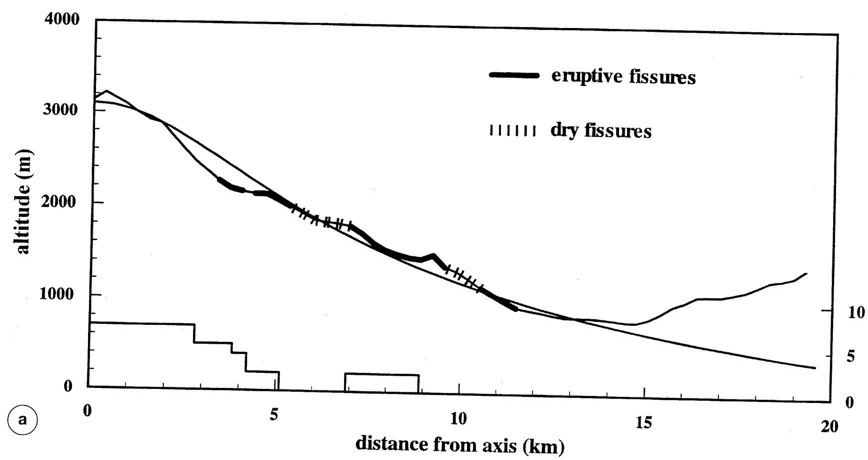

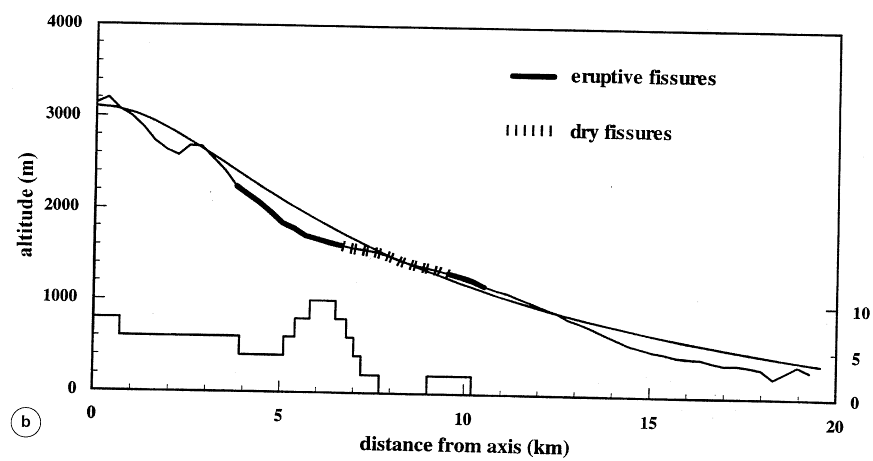

Fig. 4a,b. The 1981 (a) and the 1928 (b) fracture systems are shown in connection with the altitude of the free surface and the topography.

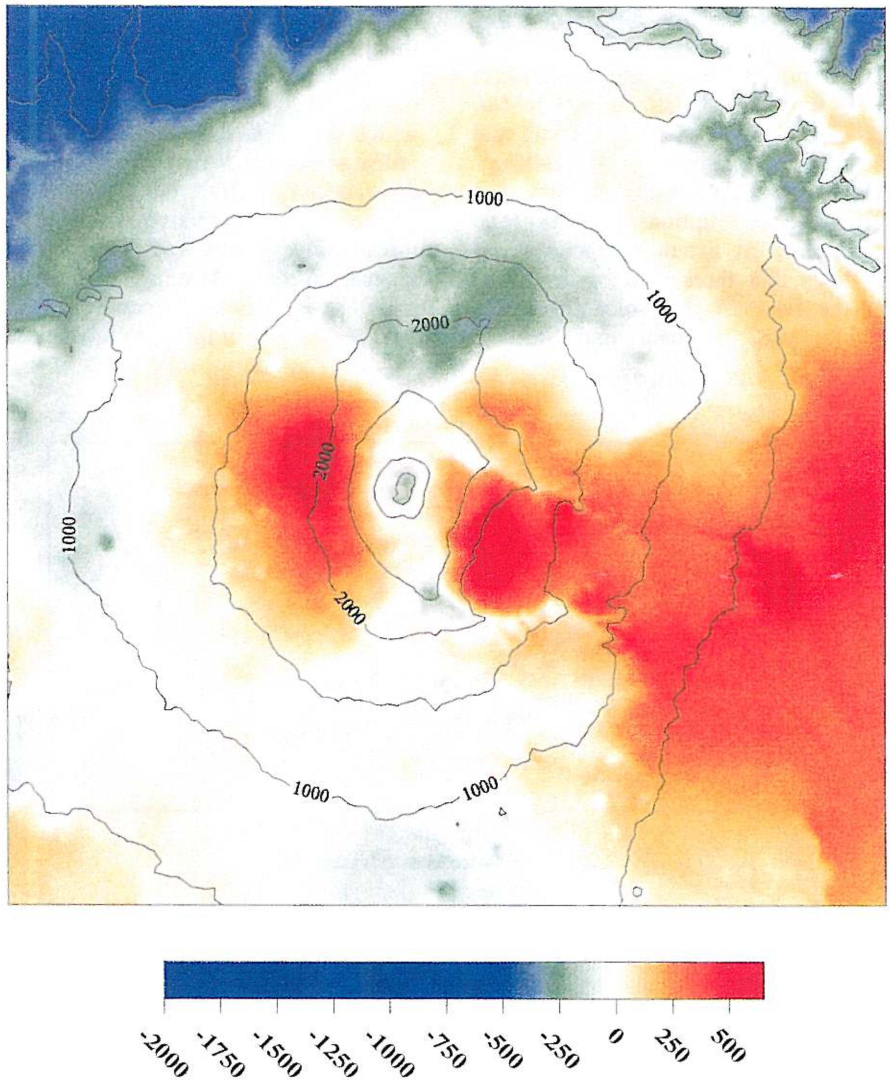

Fig. 5. The difference between the best-fit second-order free surface (computed along the SSE section) and Mt. Etna topography is shown in false colours. Over red and orange areas the free surface is higher than topography; over green and blue areas, it is lower.

showing that hazard estimates based on historical data spanning over the last 300-400 years (as they currently are) must be considered unreliable. Figure 4b shows the 1928 fracture system whose lava flow destroyed the town of Mascali and nearly reached the coast in the eastern sector. Similar lava flows took place in the low eastern flank several centuries ago, but recent flows cover the older ones hindering the identification of their feeder dyke.

It is to be noted that parameter values obtained from the second-order best-fit differ significantly from values which would be obtained from the first-order solution ($\tau = 19$, $Q = 0.32$, $z_0 = 4500$ m, $h_0 = 400$ m). Accordingly, the lower value obtained for Q in the second-order evaluation reinforces the applicability of the present perturbation approach. In spite of the differences between first-order and second-order estimates, the free surfaces appear very similar to each other and both indicate a source depth coinciding with the top of the Iblean basement plateau.

Figure 5 plots the difference (in metres) between the second-order free surface (obtained from the best fit along the SSE section) and the topography of Mt. Etna (positive values in red, negative values in blue). According to model assumptions, red areas can be interpreted as areas where magma can reach the surface if a fracture develops which connects the source region to the surface. A marked asymmetry is present between the NS and the EW sections, which is clearly related to the NS trending (approximately) rift zone. While high-altitude regions involved by eruptions are generally red (apart from the already mentioned NE rift), wide red areas are present at low altitudes in sectors where flank eruptions did not take place in the last few centuries (*e.g.*, in the eastern sector, where eruptive activity is mostly confined above 1750 m altitude).

The map shows that the actual distribution of flank eruptions is mostly governed by the heterogeneous distribution of fracture zones, more than by magma flow dynamics. However, if a fracture event, (determined, *e.g.*, by tectonic forces or by gravity instability) were to open in orange-red areas, magma pressure at the source is predicted to be sufficient to produce significant lava flows.

In particular, the map confirms that the SE sector of Mt. Etna is particularly dangerous, the free surface being always very close to the topography down to low altitudes: accordingly, if a fracture opens which connects the plumbing system to the surface, magma has enough pressure to reach the surface. Lateral eruptions on the western sector can be similarly interpreted above altitude 1200 m. Similarly, the map confirms that low-altitude flank eruptions are possible in the northern sector, as proved by the 1981 eruption discussed above. A region of major concern is however the eastern sector where the topography is systematically lower than the free surface, yet eruptions in recent centuries were mostly confined above altitude 1750 m, within the Valle del Bove caldera.

5. Conclusions

Admittedly, the model presented above is highly speculative: Mt. Etna is considered an isotropic homogeneous medium in which the complex geological setting is mostly ignored and attention is focussed on magma flow dynamics. This is not a drawback, however, since the discrepancy between model prediction and observations can lead us to better discriminate between structures that drive volcano evolution, which may disagree with model prediction (*e.g.*, the NE rift) from structures that are induced by volcano dynamics, which are compatible with the model (such as the fracture system of the 1981 eruption).

The role of the large-scale (regional) stress field has been similarly ignored: for instance, standard solutions in the framework of fracture mechanics show that dyke opening is governed by the excess of magma pressure (inside) with respect to the normal stress acting in the host rock before dyke emplacement; accordingly, a vertical dyke striking in the direction of the compressive local stress is acted on by greater overpressure than a dyke striking in the orthogonal direction. The NS elongated rift zone on Mt. Etna is in accordance with these considerations since several morphotectonic and seismic studies show that the regional stress axes in North-Eastern Sicily are oriented NS (compression) and EW (tension) (*e.g.*, Caccamo *et al.*, 1997; Cocina *et al.*, 1997).

Two further assumptions built in the model are that the source is point-like and has a fixed location in time. The latter restriction is taken into account since some authors find evidence of a slow westward migration of magmatic activity on Mt. Etna (*e.g.*, Gresta *et al.*, 1990; Borgia *et al.*, 1992). Both restrictions might be easily overcome, at least in principle, by building an extended or a moving source through the superposition of several, suitably located, point sources.

From the present speculative model however, we were able to explain many features of Mt. Etna topography and eruption distribution in the southern and northern sectors without invoking any discontinuity in local structural properties (faults, rifts, rock inhomogeneities etc.) or any pre-established path for magma migration (local fracture zones, multiple open conduits, secondary magma chambers etc.). The role of the regional stress field and the presence of extended sources will be considered in a separate paper.

Acknowledgements

M.B. wishes to thank Michele Caputo for his life-long teaching that mathematics is the natural language to understand the Earth. The authors wish also to thank A. Borgia for useful discussions. Work performed with financial contribution from MURST 40% and the Commission of European Communities (Program Environment and Climate). N.C. is supported by a fellowship under contract ENV4. CT96.0259.

REFERENCES

BEAR, J. (1976): *Dynamics of Fluids in Porous Media* (American Elsevier, New York), pp. 764.

BECKER, G.F. (1885): The geometric form of volcanic cones and the elastic limit of lava, *Am. J. Sci.*, **30**, 283-293.

BONAFEDE, M. and E. BOSCHI (1992): A porous flow model of flank eruptions on Mount Etna, *J. Volcanol. Geotherm. Res.*, **49**, 349-363.

BORGIA, A., L. FERRARI and G. PASQUARÈ (1992): Importance of gravitational spreading in the tectonic and volcanic evolution of Mount Etna, *Nature*, **357**, 231-235.

CACCAMO, D., G. NERI, A. SARAO and M. WYSS (1997): Estimates of stress directions by inversion of earthquake fault-plane solutions in Sicily, *Geophys. J. Int.*, **125**, 857-868.

CENNI, N. (1996): Flusso non confinato di un fluido in mezzi permeabili, *Tesi di Laurea in Fisica*, a.a. 1994-95, Dept. Physics, University of Bologna.

CHESTER, D.K., A.M. DUNCAN, J.E. GUEST and C.R.J. KILBURN (1985): *Mount Etna – The Anatomy of a Volcano* (Chapman and Hall, London), pp. 404.

COCINA, O., G. NERI, E. PRIVITERA and S. SPAMPINATO (1997): Stress tensor computations in Mount Etna area (Southern Italy) and tectonic implications, *J. Geodynamics*, **23**, 109-127.

CRISTOFOLINI, R., G. PATANÈ and R. RASÀ (1978): Studio morfo-strutturale del versante orientale etneo, *Mem. Soc. Geol. Ital.*, **19**, 613-620.

CRISTOFOLINI, R., R. FICHERA and G. PATANÈ (1981): Osservazioni morfo-tettoniche sul settore occidentale dell'Etna, *Geogr. Fis. Dinam. Quat.*, **4**, 55-63.

DAGAN, G. (1966): The solution of the linearized equations of free surface flow in porous media, *J. Mécanique No. 2*, **5**, 207-215.

GRESTA, S., V. LONGO and A. VIAVATTENE (1990): Geodynamic behaviour of eastern and western sides of Mount Etna, *Tectonophysics*, **179**, 81-92.

GUEST, J.E. and J.B. MURRAY (1979): An analysis of hazard from Mount Etna volcano, *J. Geol. Soc. Lond.*, **136**, 347-354.

LACEY, A., J.R. OCKENDON and D.L. TURCOTTE (1981): On the geometrical form of volcanoes, *Earth Planet. Sci. Lett.*, **54**, 139-143.

LO GIUDICE, E., G. PATANÈ, R. RASÀ and R. ROMANO (1982): The Structural framework of Mount Etna, *Mem. Soc. Geol. Ital.*, **23**, 125-158.

MILNE, J. (1878): On the form of volcanoes, *Geol. Mag.*, **15**, 337-345.

MILNE, J. (1879): Further notes on the form of volcanoes, *Geol. Mag.*, **16**, 506-514.

POLUBARINOVA-KOCHINA, P.YA. (1962): *Theory of Ground Water Movement* (Princeton University Press, Princeton, N.J.), pp. 613.

RASÀ, R., R. ROMANO and E. LO GIUDICE (1982): A structural survey of Mount Etna on a morphological basis, *Mem. Soc. Geol. Ital.*, **23**, 117-124.

ROMANO, R. (1982): Succession of volcanic activity in the Etnean area, *Mem. Soc. Geol. Ital.*, **23**, 27-48.

ROMANO, R. and C. STURIALE (1982): The historical eruptions of Mount Etna (volcanological data), *Mem. Soc. Geol. Ital.*, **23**, 75-97.

SHTEYNBERG, G.S. and T. SOLOV'YEV (1976): The shape of volcanoes and the position of subordinate vents, *Izv. Earth Phys.*, **5**, 83-84.

WADGE, G. and P. FRANCIS (1982): A porous flow model for the geometrical form of volcanoes – critical comments, *Earth Planet. Sci. Lett.*, **57** 453-455.

WILLIAMS, H. and A.R. MCBIRNEY (1979): *Volcanology* (Freeman, Cooper, San Francisco) pp. 397.